

The binarity of Galactic dwarf stars along with effective temperature and metallicity

Shuang Gao^{1★}, He Zhao¹, Hang Yang¹, Ran Gao¹

¹*Department of Astronomy, Beijing Normal University, Beijing 100875, China*

Accepted XXX. Received YYY; in original form ZZZ

ABSTRACT

The fraction of binary stars (f_b) is one of most valuable tool to probe the star formation and evolution of multiple systems in the Galaxy. We focus on the relationship between f_b and stellar metallicity ([Fe/H]) by employing the differential radial velocity (DRV) method and the large sample observed by the Large Sky Area Multi-Object Fiber Spectroscopic Telescope (LAMOST). Main-sequence stars from A- to K-types in the third data release (DR3) of LAMOST are selected to estimate f_b . Contributions to a profile of DRV from radial velocity (RV) error of single stars (σ_{RV}) and orbital motion of binary stars are evaluated from the profile of DRV. Finally, we employ 365,911 stars with randomly repeating spectral observations to present a detailed analysis of f_b and σ_{RV} in the two-dimensional (2D) space of T_{eff} and [Fe/H]. The A-type stars are more likely to be companions in binary star systems than other stars. Furthermore, the reverse correlation between f_b and [Fe/H] can be shown statistically, which suggests that f_b is a joint function of T_{eff} and [Fe/H]. At the same time, σ_{RV} of the sample for different T_{eff} and [Fe/H] are fitted. Metal-rich cold stars in our sample have the best RV measurement.

Key words: binaries: close — binaries: spectroscopic — galaxy: disc — stars: formation — stars: statistics

1 INTRODUCTION

Binary stars (and multiple systems) in the Milky Way play a significant role from stellar evolution to supernova (Duchêne & Kraus 2013). However it is very challenging to identify a binary system from single stars and to determine physical parameters of the binary stars (mass ratios¹ q , orbital periods P , and eccentricities e) in different stellar populations and Galactic environments.

The f_b in different environments and types were investigated in the last decades. Duquennoy & Mayor (1991) and Raghavan et al. (2010) found that f_b for solar-type stars is about 45 per cent generally. More particularly, they reported that the f_b increases from 40 per cent for sub-solar to 60 per cent for super-solar stars. For stars with lower masses ($< 0.5 M_\odot$), Dieterich et al. (2012) reported the f_b is only about 26 per cent. On the other hand, OB stars likely have much higher f_b . The f_b of stars with $M > 5 M_\odot$ is larger than 70 per cent (Sana et al. 2012). Many above studies have been conducted the f_b as a steep and monotonic function of stellar

mass. For selected MS stars, the relationship can be considered as a function of the f_b and stellar effective temperature T_{eff} .

The radial velocity (RV, v_r) of the star can be determined by running a pipeline of spectra data. A single star has the constant RV with observed uncertainty σ_{RV} , meanwhile binary star systems show systematic shifts in RV caused by the orbital motion of each companion. RV changes help distinct binaries from single stars. The differential RV (DRV, Δv_r) method makes use of twice RV measurements to obtain the profile of DRV, that is the sum of two components of single and binary stars.

Recently, several investigators have studied f_b that suffers from stellar metallicity. Gao et al. (2014) reported that the metal-poor stars are likely to possess a close binary companion than metal-rich population. The f_b in Galactic halo and thick disk are 20 to 30 per cent larger than thin disk for close binaries with $P < 1000$ d. This general trend was supported by Yuan et al. (2015) by stellar locus outlier method. Due to limitations of the number of sources and time spans, the f_b estimated by these work have relatively large uncertainties, and f_b of the Galactic thick disk by Yuan et al. (2015) is inconsistent with Gao et al. (2014)'s result. Besides, results of f_b from these work are dominated

★ E-mail: sgao@bnu.edu.cn

¹ The q is defined as the ratio of the secondary to primary mass, i.e. $q \equiv M_2/M_1$

by wider-period binaries. [Hettinger et al. \(2015\)](#), however, revealed the multiplicity of short-period binaries with the sub-exposures data archived in the Sloan Digital Sky Survey (SDSS). The investigation found that metal-rich disk stars are 30 per cent more likely to have companions with $P < 12$ d than metal-poor halo stars. Therefore the relationship between f_b and stellar metallicity ($[\text{Fe}/\text{H}]$) is still too far to be solved entirely.

Large spectral surveys provide opportunities to obtain physical parameters, such as RV, of a massive amount of stars. To access f_b by using DRV method, large sample with repeat RV observations during different epochs is necessary.

LAMOST sample and data reduction are described in Section 2. Our analysis method is presented in Section 3. The results are presented and discussed in Section 4. A conclusion is given in Section 5.

2 DATA

The Large Sky Area Multi-Object Fiber Spectroscopic Telescope (also known as LAMOST, see [Cui et al. 2012](#); [Zhao et al. 2012](#), for the overview) is an optical telescope operated by National Astronomical Observatories of China (NAOC). It is special reflecting Schmidt system with 4-meter diameter and 4000 fibres in a large field of view (FOV) of 20 deg² in the sky. The LAMOST Experiment for Galactic Understanding and Exploration (LEGUE) survey of Milky Way stellar structure observed spectra of stars and released the third data (DR3) recently², containing 5,755,126 spectra and 3,178,057 *AFGK* stars with stellar parameters in DR3 catalogue totally. Those stars were observed from 2011 October 24 to 2015 May 30.

DR3 catalogue gives the stellar physical parameters T_{eff} , $[\text{Fe}/\text{H}]$, and surface gravity ($\log g$) of 3,178,057 A, F, G and K-type stars based on template match method ([Wu et al. 2011, 2014](#)). The determination of these parameters consistently adopts the cross-correlation approach with a simultaneous linear combination of single stellar templates ([Luo et al. 2012](#)).

We identify 365,911 stars that were observed twice from almost 3.2 million sources. The RV of two epochs of each star can be obtained via self-matching of the catalogue. Among these stars, our sample is selected by using the following criteria:

- $\text{SNR}_g > 20$;
- $-300 \text{ km s}^{-1} < \Delta v_r < 300 \text{ km s}^{-1}$;
- $4000 \text{ K} < T_{\text{eff}} < 8000 \text{ K}$;
- $-1.0 \text{ dex} < [\text{Fe}/\text{H}] < 0.5 \text{ dex}$.

Where SNR_g is signal-noise-ratio at g band and Δv_r is defined as the difference between two RV observations $v_1 - v_2$ to select MS dwarf stars, the $\log g$ is constrained sectionally following [Liu et al. \(2014\)](#):

- $\log g > 4.0$, if $T_{\text{eff}} < 5500 \text{ K}$;
- $\log g > 3.5$, if $5500 \text{ K} < T_{\text{eff}} < 6000 \text{ K}$;
- $\log g > 3.0$, if $T_{\text{eff}} > 6000 \text{ K}$.

² <http://dr3.lamost.org>

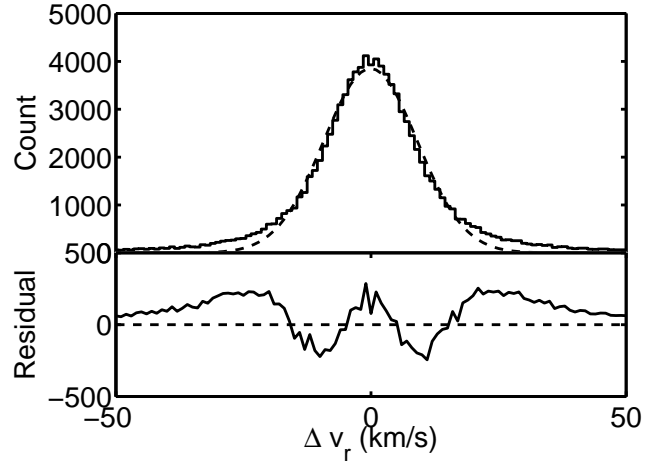


Figure 1. The profile of DRV and fitting. *Top*: The distribution of Δv_r of the entire sample. The solid and dashed curve is the histogram of observed data and a Gaussian fitting result, respectively. *Bottom*: The residual error of data and Gaussian fitting. The x-axis is limited within -50 to 50 km s^{-1} to obtain a more distinct presentation. The bin size of x-axis is 1 km s^{-1} .

Further, the sources observed on the same nights are excluded because so small time span cannot generate significant enough RV shift of binary stars. Besides, observations in the same nights may underestimate random errors of RVs. Finally, our sample contains 303,803 quality dwarf stars with their parameters pairs from repeated observations.

The general distribution of Δv_r shows a non-Gaussian symmetric profile as Figure 1. One Gaussian function cannot fit our data even though the profile of Δv_r is similar with a bell-shaped curve. The significant residual errors between data and one Gaussian fit imply that only random error caused by single stars observation is inadequate to explain Δv_r data.

The pipelines of LAMOST have a validation with SDSS data. The stellar parameters in our sample have been determined by an automatic process based on [Wu et al. 2011](#), 's method. [Gao et al. \(2015\)](#) found that the standard deviations of 110 K, 0.11 dex and 4.91 km s^{-1} , for T_{eff} , $[\text{Fe}/\text{H}]$ and RV. According to the work of [Ren et al. \(2016\)](#), LAMOST's T_{eff} and $[\text{Fe}/\text{H}]$ have the deviation of about 100 K and 0.1 dex in Kepler field, respectively. The pipeline and these independent validations confirm the accuracy of T_{eff} and $[\text{Fe}/\text{H}]$ for dwarfs, which is matching the coverage of parameters in our sample. Our analysis is based on the sample and the errors of stellar parameters. The unprecedented size of the sample with reliable errors help distinguish binary stars from single stars and draw the potential trend between the binarity and stellar parameters.

3 METHOD AND MODEL

The spectral observations of two epochs may obtain different v_r of a star. These mechanisms work to a shift of v_r : pulsating star, observed random error, and orbital motion of the binary system. We ignore the first one for MS stars in our

mass range because the tiny deviation of MS stars cannot be uncovered by an observed accuracy of km s^{-1} -size. The latter two mechanisms change observed RV of stars at two epochs with the different way: all RV data suffer observed random error but orbital motion only affects a fraction of stars, that is our scientific goal f_b . We develop a simple method to estimate respective contributions of the last two mechanisms to some given sample without known f_b and σ_{RV} .

A sample with a mixture of single and binary stars from observed data, like LAMOST spectral database, needs to be revealed the ratio of the contributions caused by two components. Pure single stars and binary stars components are derived via simulations of our model that involved random error and Kepler's orbital motion.

3.1 Model and Simulation

For a single star, observed v_r suffers random error σ_{RV} . We assume that the Δv_r between two epochs follows a Gaussian distribution with an average value of 0 and standard deviation of $\sqrt{2}\sigma_{RV}$:

$$\Delta v_r^{(s)} = v_1^{(s)} - v_2^{(s)} \sim N(0, \sqrt{2}\sigma_{RV}), \quad (1)$$

where superscript (s) represents single star and (b) in the following text is for binary stars.

For a binary star system, besides random error, observed v_r changes with the orbital motion of companions. The profile of $\Delta v_r^{(b)}$ is so complicated that we have to describe it by using a model that involves P , q , the mass of primary star M_1 and other orbital parameters.

Given P , M_1 and q , the maximum shift K of RV of the primary star can be calculated based on the Keplerian two-body law as follows equation:

$$\frac{K}{\text{km s}^{-1}} = 212.6 \left(\frac{M_1}{M_\odot}\right)^{\frac{1}{3}} \left(\frac{P}{\text{d}}\right)^{-\frac{1}{3}} q(1+q)^{-\frac{2}{3}} \frac{\sin i}{\sqrt{1-e^2}}, \quad (2)$$

where i and e are orbital orientation and eccentricity, respectively. The basic distributions of parameters are assumed as follows forms:

- Most e are close to 0. We adopt circular orbit $e = 0$ to simplify our calculation.
- The distribution of P follows Raghavan et al. (2010). A log-normal distribution is used to draw random mock P in our method.
- The distributions of i and q follow uniform functions.

The models with different f_b are shown as Figure 2. The mock Δv_r derived by our model depends on M_1 , which is determined based on T_{eff} and $[\text{Fe}/\text{H}]$ in sample by theoretical stellar isochrones (Girardi et al. 2000). In Section 3.2, the T_{eff} and $[\text{Fe}/\text{H}]$ of each box is used to estimate the M_1 for mock binary model. In the other words, each box has a set of model with different M_1 and corresponding mock Δv_r .

Considering orbital phase of two observed epochs and observed random error, we have

$$\Delta v_r^{(b)} = v_1^{(b)} - v_2^{(b)} \sim N(K(\cos \phi_1 - \cos \phi_2), \sqrt{2}\sigma_{RV}), \quad (3)$$

which K is the amplitude of RV variation, and ϕ is the phase of each observation time. The Δv_r due to binary stars follows a Gaussian profile with average of $K(\cos \phi_1 - \cos \phi_2)$ and standard deviation of $\sqrt{2}\sigma_{RV}$.

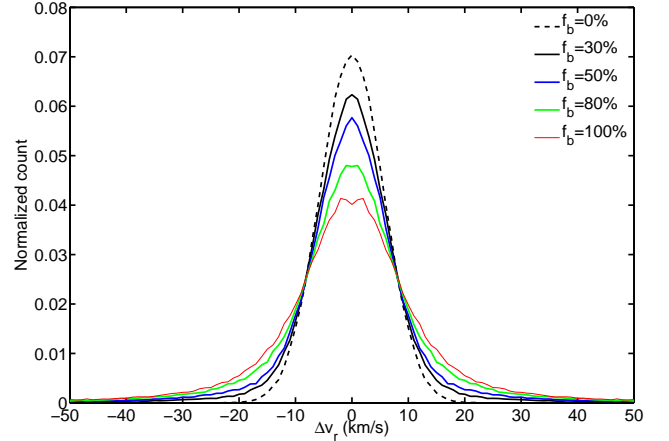


Figure 2. The profile case of Δv_r derived by our model with different f_b . Five curves represent five different input values of f_b : 0, 30, 50, 80, and 100 per cent, respectively. The M_1 is equal to $1 M_\odot$. The x- and y-axis is Δv_r and normalised count. These profiles don't consider observed errors.

If a profile of Δv_r can be explained by a Gaussian distribution with random error $\sqrt{2}\sigma_{RV}$, this profile is considered to be full of single stars. If $\Delta v_r^{(b)}$ can depict a profile of Δv_r , it will be considered to be f_b of 100 per cent. The optimal combination of f_b and σ_{RV} of a sample with given Δv_r distribution should be fitted at the same time.

To test our method, we generate mock samples with known input f_b using model described above and then to simulate the process of f_b estimation. The simulated sample contains 10,000 sources with different given input f_b from 0 to 100 per cent. The estimation process of the f_b (and σ_{RV}) for each input f_b is repeated 100 times to obtain their uncertainties. The f_b of mock samples are estimated as the showing of Figure 3. The M_1 is $1 M_\odot$ and other orbital parameters adopt sets of model mentioned above. The completeness of estimation of f_b is always larger than 95 per cent for various input f_b .

For real observed sample, we run the process that is similar to above test. The 10,000 mock sources with 100% binary star component are prepared before the fitting process. The normalised profile of $\Delta v_r^{(b)}$ is calculated based on mock binary star model. These “binary stars” are our binary component whose profile is used to fit the DRV of the real sample. The f_b and σ_{RV} are determined by fitting the contribution rates of mock binary star sample and Gaussian error.

3.2 T_{eff} and $[\text{Fe}/\text{H}]$

To deal with our sample in which stellar mass need to be determined before a fitting process of f_b . Based on stellar isochrones of MS stars, the M_1 is estimated via T_{eff} and T_{eff} in the sample. In our sample, maximum M_1 is below to $2 M_\odot$.

Gao et al. (2014) and Yuan et al. (2015) divided field stars into three populations with $[\text{Fe}/\text{H}]$ of the thin disk, thick disk, and halo in the Milky Way. The larger sample allows us to investigate f_b along with $[\text{Fe}/\text{H}]$ in a more detailed way.

Combining above two aims, the sample is divided into

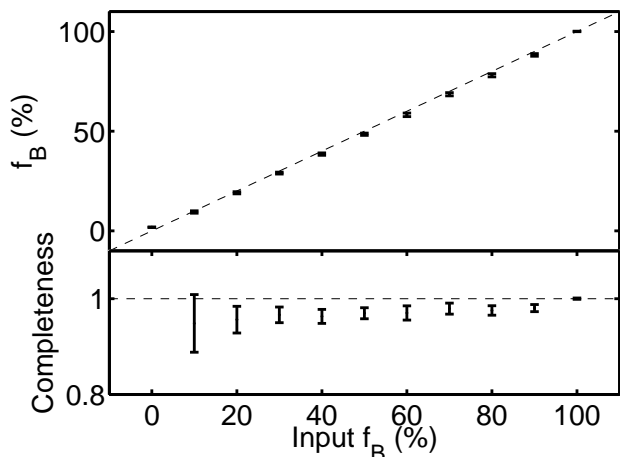


Figure 3. The simulation and test of our method and binary model. *Top:* the comparison between input f_b and derived f_b . The dashed line is 1 : 1 for reference. Most error bars are smaller than the markers in the figure, so they are not very obvious. *Bottom:* the y-axis is converted into completeness that is defined as the ratio of derived to input f_b . The dashed line marks 100% level.

20×20 box along with T_{eff} and $[\text{Fe}/\text{H}]$. Considering the errors (~ 100 K, ~ 0.1 dex) for T_{eff} and $[\text{Fe}/\text{H}]$ (Gao et al. 2015; Ren et al. 2016), the two-dimensional (2D) distribution in 20×20 box is smoothed by a 2×2 box. In each $(T_{\text{eff}}, [\text{Fe}/\text{H}])$ box, the stellar mass M_1 is considered independently when we fit f_b and σ_{RV} .

Similar to simulation and testing method, fitting process is repeated 100 times to obtain error bars of f_b and σ_{RV} . If star count is too small, the f_b and σ_{RV} fitting cannot output credible results. We don't run the fitting process if the star count in a $(T_{\text{eff}}, [\text{Fe}/\text{H}])$ box is less than 100.

4 RESULT AND DISCUSSION

As a showing of the bottom panel in Figure 4, edge regions of the colourful part have relative larger f_b error. Especially, the f_b errors at the left and right bottom corners are larger than 10 per cent. So large uncertainty makes f_b of corresponding $(T_{\text{eff}}, [\text{Fe}/\text{H}])$ boxes short of credibility.

The credibilities of the leftmost and rightmost columns of boxes in Figure 4 should be doubted due to relative large f_b uncertainty. Except that, the f_b increases along with raised T_{eff} . The f_b changes from ~ 20 to ~ 50 per cent when T_{eff} increases from 4000 to 7500 K. The relationship between f_b and T_{eff} won't surprise us because of past observational results (Raghavan et al. 2010, and references therein). Stars with higher temperature are massive to keep their companions. For metal-rich sample (the upper part of upper left panel of Figure 4), the f_b increases from ~ 30 to ~ 60 per cent throughout the T_{eff} . These results are consistent with previous work (Gao et al. 2014; Raghavan et al. 2010). Not only is shown that we have confirmed the relationship between f_b and T_{eff} , but also the detailed gradual change of f_b with T_{eff} .

In Figure 4, f_b changes in two directions: T_{eff} and $[\text{Fe}/\text{H}]$. The f_b increases when $[\text{Fe}/\text{H}]$ decreases in Figure 4 even though edge region of colourful boxes have large uncertainty.

As showing of Figure 4, the f_b is close to 50 per cent for $[\text{Fe}/\text{H}] < -0.5$ dex. Compared with metal-poor stars, the f_b is only between 20 and 30 per cent for near-zero $[\text{Fe}/\text{H}]$. The f_b in halo and thick disk population is almost higher twice than thin disk.

Metal-rich stars with the same mass have slightly lower temperature due to higher opacity. Thus metal-rich stars with the same temperature have a little higher stellar mass. The relationship between f_b and $[\text{Fe}/\text{H}]$ needs to be explained by reasons beyond stellar mass.

Metal rich and K-type stars are most unlikely to have companions. Figure 4 shows a gradient of f_b from top-left to bottom-right corner. In the area of $4500 \text{ K} < T_{\text{eff}} < 7000 \text{ K}$ and $-0.75 \text{ dex} < [\text{Fe}/\text{H}] < 0.3 \text{ dex}$, f_b rises 10 per cent if T_{eff} increases ~ 400 K and $[\text{Fe}/\text{H}]$ decreases ~ 0.2 dex.

Reasons for the relationship between the f_b and $[\text{Fe}/\text{H}]$ need to be investigated carefully. Why metal abundance affects formation or evolution of binary systems? What roles do time and stellar life span play in this relationship? A few reasons can be listed as follows to explain above trends:

- The formation of metal-poor binary stars intrinsically are easier than metal-rich binaries.
- The f_b is uniform in different environments originally, but high $[\text{Fe}/\text{H}]$ leads to complicated interactions of binary systems, which loses companions.

In part of T_{eff} and $[\text{Fe}/\text{H}]$ boxes, small sizes of spectral sample produce large relative uncertainties. To confirm the significant and robust of the results from LAMOST DR3, we need a larger spectral sample with repeat observations, which provides substantial evidence for trends of the f_b .

The distribution of P for $M_1 < 1.5 M_{\odot}$ keeps a certain trend (Duchêne & Kraus 2013). For $M_1 > 1.5 M_{\odot}$, $T_{\text{eff}} > 7000 \text{ K}$. In each panel of Figure 4, these intermediate-mass stars only affect two strips of the rightmost side in the colourful areas. And most influenced boxes have been removed out of our final discussion due to their small size of available sample. It is a remarkable fact that the distribution of q values is assumed to be flat between 0.0 to 1.0, but a more complicated profile of q maybe reduce the ratio of massive secondary stars, which causes smaller v_r shift due to the relative orbital motion. Thus the f_b based on observed Δv_r could be higher generally when we adopt a non-flat q distribution.

5 CONCLUSIONS

We deal with a spectral sample containing 365,911 pairs of stellar parameters from repeat observations of LAMOST. The profile of DRV of selected MS stars is used to fit the f_b and σ_{RV} in a 2D space of T_{eff} and $[\text{Fe}/\text{H}]$. The fitted two components contain artificial binary sample based on Keplerian orbital motion and Gaussian errors of RV.

We reveal a 2D trend of f_b with T_{eff} and $[\text{Fe}/\text{H}]$. We suggest that the relationship between f_b and T_{eff} (stellar mass) can be confirmed, but one more factor, $[\text{Fe}/\text{H}]$, affects the f_b in our sample. Metal-poor hot stars are more likely to have a close binary companion than metal-rich cool stars. Meanwhile, metal-rich cool stars have the best RV measurements. The general σ_{RV} is about 3.0 to 3.5 km s^{-1} .

The deeper understanding of the relationship between

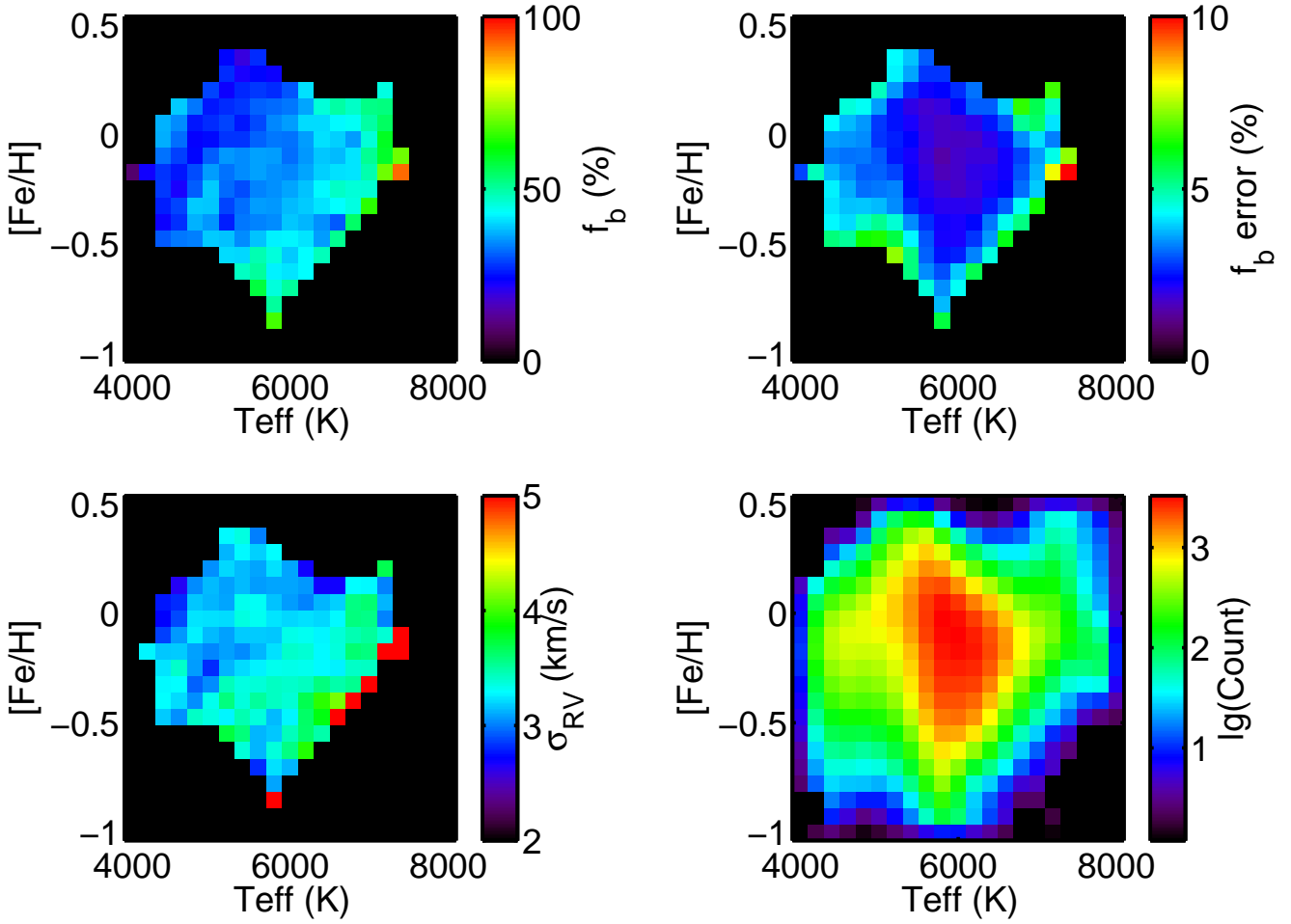


Figure 4. *Upper left:* The distribution of the f_b in the sample. The x-axis is the T_{eff} from 4000 to 8000 K and the y-axis is the $[\text{Fe}/\text{H}]$ from -1.0 to 0.5 dex. The f_b , for each $(T_{\text{eff}}, [\text{Fe}/\text{H}])$ sub-sample, is colour-coded by a linear scale from 0 to 100 per cent. The black region is a lack of enough data (at least 100 sources). *Upper right:* The distribution of the f_b error in the sample. The x-axis and the y-axis are the same with the left top panel. The f_b error is colour-coded linearly from 0 to 10 per cent. *Lower left:* The distribution of the σ_{RV} . The axis is the same with upper panels. The σ_{RV} is colour-coded by a linear scale from 2 to 5 km s^{-1} . *Lower right:* The distribution of the star count in the sample. The axis is the same with other panels. The star count is colour-coded by a logarithmic scale from 1 to 3000.

close binary systems and their $[\text{Fe}/\text{H}]$ requires detailed further study and more spectral data.

ACKNOWLEDGEMENTS

We would like to thank the anonymous reviewer for his/her comments, which significantly improved the paper. Authors are supported by grants No. 11503002 and 11533002 from the National Natural Science Foundation of China (NSFC). Authors thank helpful discussions with Prof. Biwei Jiang and Dr. Haibo Yuan.

REFERENCES

Cui X. Q., Zhao Y. H., Chu Y. Q. et al., RAA, 12, 1197
 Dieterich S. B., Henry T. J., Golimowski D. A. et al., 2012, AJ, 144, 64
 Duchêne G. & Kraus A., 2013, ARA&A, 51, 269
 Duquennoy A. & Mayor M., 1991, A&A, 248, 485
 Gao H., Zhang H.-W., Xiang M.-S. et al., 2015, RAA, 155, 2204

Gao S., Liu C., Zhang X. et al., 2014, ApJ, 788, 37L
 Girardi L., Bressan A., Bertelli G. et al., 2000, A&AS, 141, 371
 Hetteringer T., Badenes C., Strader J. et al., 2015, 806, 2
 Liu C., Deng L. C., Carlin J. L. et al., 2014, ApJ, 790, 110
 Luo A., Zhang H. T., Zhao Y. H. et al., 2012, RAA, 12, 1243
 Raghavan D., McAlister H. A., Henry T. J. et al., 2010, ApJS, 190, 1
 Ren A., Fu J., De Cat P. et al., 2016, ApJS, 225, 28
 Sana H., de Mink S. E., de Koter A. et al., 2012, Science, 337, 444
 Wu Y., Luo A., Li H. et al., 2011, RAA, 11, 924
 Wu Y., Du B., Luo A. et al., 2014, IAUS, 306, 340
 Yuan H., Liu X., Xiang M. et al., 2015, ApJ, 799, 135
 Zhao G., Zhao Y. H., Chu Y. Q. et al. 2012, RAA, 12, 723

This paper has been typeset from a $\text{\TeX}/\text{\LaTeX}$ file prepared by the author.